Biophysical Chemistry 19 (1984) 113–120
Elsevier

BPC 00833

MODELS FOR THE ANALYTICAL ULTRACENTRIFUGE BEHAVIOR OF *HELIX POMATIA* α-HEMOCYANIN

II. SIMULATIONS OF REACTING MICROHETEROGENEOUS HEMOCYANIN

Mei-Sheng TAI ** and Gerson KEGELES *

Section of Biochemistry and Biophysics, Biological Sciences Group, The University of Connecticut, Storrs, CN 06268, U.S.A.

Received 4th October 1983
Accepted 28th October 1983

Key words: Stopped-flow dilution amplitude; Hemocyanin sedimentation; Microheterogeneity; Whole-half molecule reequilibration; Fractionation simulation

Simulations for the moving-boundary ultracentrifuge behavior of *Helix pomatia* α-hemocyanin have been developed, based on modification of published models. In the present treatment, it has been assumed that the protein system is extensively microheterogeneous, with respect to its whole-half molecule reactivity. It has also been assumed that all such association and dissociation reactions can proceed to equilibrium in a time appreciably shorter than that which would be required to separate nonreacting half molecules from nonreacting whole molecules. Predictions based on this model agree well with reported experimental findings of nonequilibration of fractionated material, apparent independence of whole-to-half molecule concentration ratios on total concentration in sedimentation experiments, and stopped-flow dilution reactivity over a wide range of sedimentation coefficients.

1. Introduction

As indicated in the companion paper [1], both the microheterogeneity model [2] and the reacting system-incompetent whole molecule model [3] for the sedimentation behavior of *Helix pomatia* α-hemocyanin are improved by taking into account reactivity of material responsible for the development of the raised baseline region between nominal '60 S' and '100 S' Schlieren peaks. In doing so, we will continue to maintain the conviction that in the absence of very slow interaction between half and whole molecules [4], and in the absence of strongly influencing ligand-binding interactions [5], no resolution can be achieved in moving boundary experiments [6], between separate peaks due to reacting half and whole molecules. At a given concentration, any shift of peak position in the sedimentation diagram must then be attributed entirely to variation in the formation constant of whole molecules from halves, assuming instantaneous reequilibration between species. Each subspecies has been assigned a characteristic formation constant for whole molecules, and cross-reaction between subspecies having different formation constants has been assumed to be absent. The behavior of hypothetical samples taken from moving boundary sedimentation fractionations has been predicted for both resedimentation and for stopped-flow dilution examinations, and these have been compared with the most nearly related experiments. This type of model succeeds in generating the following predictions: (1) material is distributed in two major peaks, sedimenting near 60 S and 100 S, with a very appreciable amount of

* To whom correspondence should be addressed at: 6 Oakwood Dr., Stafford Springs, CT 06076, U.S.A.
** Present address: Creative Biomolecules, Hopkinton, MA, U.S.A.

0301-4622/84/$03.00 © 1984 Elsevier Science Publishers B.V.

material raising the baseline region between the two major peaks; (2) independent of total concentration, material, as judged by sedimentation analysis, does not transfer between 60 S and 100 S peaks; (3) fractions which are either enriched in or depleted of species generating one of the major sedimentation peaks do not reequilibrate even after long storage; (4) there is reactivity in stopped-flow dilution over a wide range of sedimentation coefficients.

2. Simulation

If all of these interactions are subunit-specific, then a good overview of the possible situation is supplied by examining the asymptotic patterns predicted by Gilbert [6] for the effects of changing equilibrium constants, at constant concentration. This is shown in fig. 1. Each individual pattern shown is predicted from one value of the formation constant, K, for whole molecules from halves, so that each pattern represents the asymptotic moving boundary sedimentation behavior of one individual homogeneous whole-half molecule reacting species. The successive K values selected for the computations of these patterns are indicated in table 1. It is seen that if half molecules alone move at 60 S and whole molecules alone move at 100 S, a broad range of equilibrium constants, corresponding to the broad microheterogeneity postulated by Konings et al. [7], Siezen and Van Driel [2], and Engelborghs and Lontie [8], can effectively distribute material anywhere between 60 S and 100 S. This was already suggested by Engelborghs and Lontie [8]. Thus, as already indicated in previous studies [3,9], a composite system containing numerous species with a distribution of K values might be hypothesized, to explain the observed ultracentrifuge behavior. If it is to be acceptable, this model must also be required to satisfy the peculiar apparent independence of pattern resolution on total protein concentration.

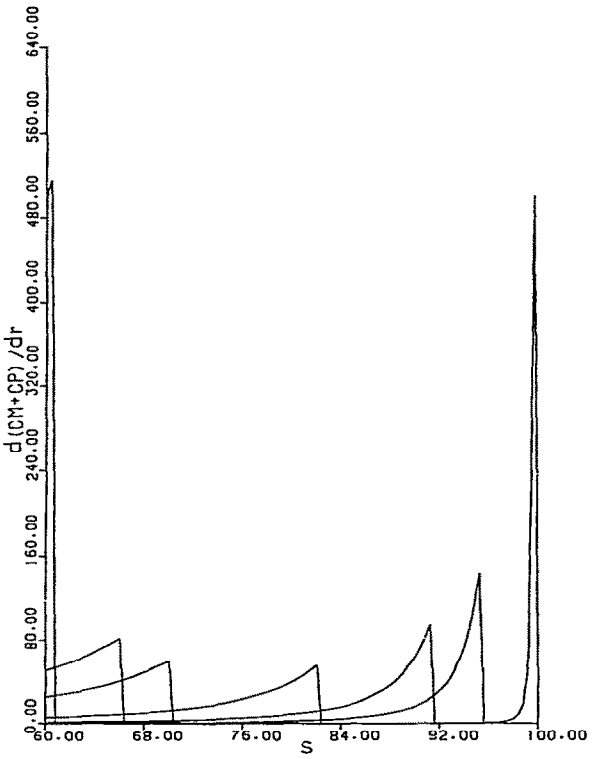

Fig. 1. Gilbert simulations [6] for rapidly reacting monomer-dimer systems with different formation constants. The concentration gradient is plotted against the sedimentation coefficient, assuming s values of 60 and 100 S for monomer and dimer, respectively. Each species is assumed to be at an original concentration of 10 g/l. The values of the formation constants increase from left to right in the figure, according to table 1.

To bring these ideas more into line with some reasonable guesses as to the actual composition of α-hemocyanin, and the effects of such interactive microheterogeneity on sedimentation patterns,

Table 1

Thermodynamic dilution reaction amplitudes

K (l/g)	0.001	0.01	0.02	0.1	0.5	2.0	1000
$\Delta M_w/M_w$	9.516×10^{-4}	6.543×10^{-2}	9.49×10^{-3}	1.236×10^{-2}	8.53×10^{-3}	4.938×10^{-3}	2.488×10^{-4}

separations, and reactivity in stopped-flow dilution, we have chosen a few examples of postulated mixtures, and analyzed them with the countercurrent distribution analog of moving boundary sedimentation [10], as modified to include dissociation effects due to hydrostatic pressure [11]. In this way, we can fairly readily simulate the ultracentrifuge behavior of a moderately complex microheterogeneous mixture. We are able to predict not only what its analytical sedimentation behavior should be, but also what kind of fractionation results one could ideally expect, as well as the overall amplitudes to be expected from such isolated fractions, when subjected to stopped-flow dilution experiments employing a light-scattering detector. As will be seen below still another dimension of complexity is involved when one wishes to discuss not only the total overall amplitude of the light-scattering response to dilution, but, in addition, the time scale of such experiments.

In table 1 are shown thermodynamic stopped-flow dilution light-scattering amplitudes for the identical systems whose asymptotic sedimentation patterns [6] are shown in fig. 1. These are calculated according to the relation [12]

$$\Delta M_w / M_w = (\Delta c/c)\alpha(1-\alpha)/(2-\alpha)^2 \qquad (1)$$

where M_w is the weight-average molecular weight. The degree of dissociation α is related to the formation constant K and the concentration c by the usual relationship

$$K = (1-\alpha)/c\alpha^2 \qquad (2)$$

Each system is assumed to be at an initial concentration of 10 g/l, and is assumed to be diluted by 10%. It is seen that, although the systems having extreme values of the equilibrium constant show small predicted stopped-flow dilution amplitudes, every system is nevertheless a reacting system. The largest amplitudes are predicted for systems with intermediate equilibrium constant values, but it should be pointed out that the quantitative comparison shown in table 1 will change when the assumed value of the total concentration is changed. The maximum amplitude occurs when $\alpha = 2/3$ [12]; by eq. 2, this means that the maximum amplitude occurs for $Kc = 3/4$. The entire effect of microheterogeneity on dilution

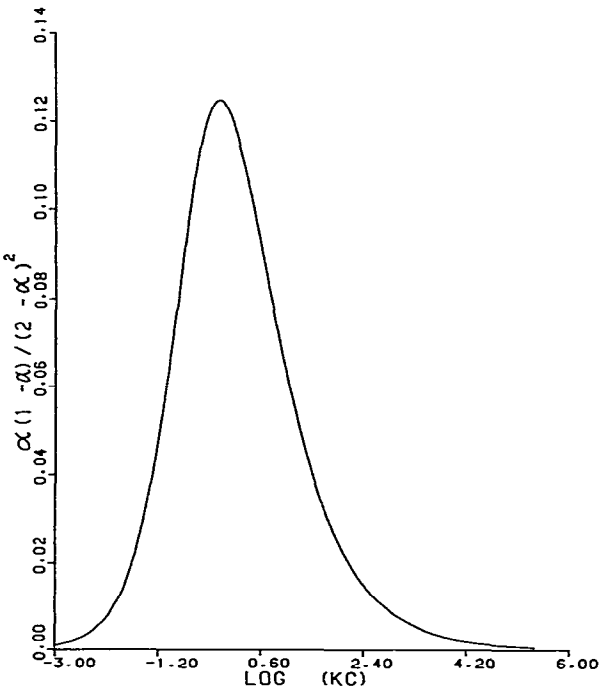

Fig. 2. Thermodynamic dilution reaction amplitude (eq. 1) versus common logarithm of the product Kc (eq. 2).

reactivity, and implicitly on the ability of species to reequilibrate during or subsequent to ultracentrifugation, is further illustrated by fig. 2. Here the thermodynamic dilution reaction amplitude, given by eq. 1, is plotted against the common logarithm of the product Kc, which is the usual function of the degree of dissociation α shown in eq. 2. It should be emphasized that this is not simply a mathematical relationship: in a microheterogeneous system, different abscissa values at fixed concentration represent separate species. A closely related discussion of the effects of microheterogeneity on sensitivity to dilution has been presented by Van Holde et al. [13]. It is particularly interesting to note the huge range over which whole molecules are thermodynamically competent to exhibit effects of dissociation. An 'incompetent' whole molecule might have to be defined as one whose product of Kc is of the order of magnitude 10^4 or larger.

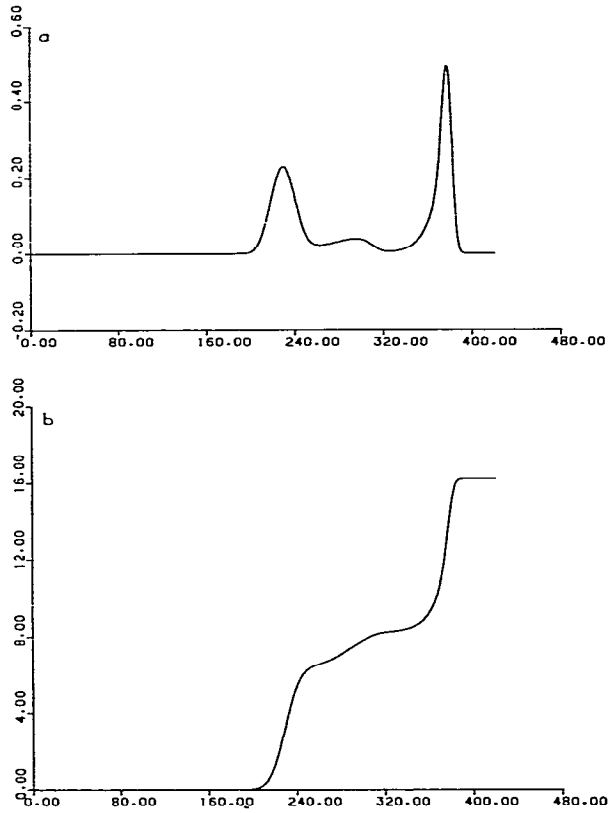

Fig. 3. Countercurrent analog simulation of the sedimentation of a mixture of four species. Dimerization formation constant values are 0.001, 0.154, 10 and 1000 l/g. Individual concentrations are 6, 2, 2 and 6 g/l, respectively. Increase in volume, 141.62 ml/mol dimer. Respective countercurrent distribution analog partition coefficient values are 1.308 and 17.07 for halves and wholes throughout these computations. The abscissa represents tube number in the analog, which is, for the computed 400 transfers, very closely equal to 4-times the sedimentation coefficient. (a) Gradient diagram, (b) concentration diagram.

In fig. 3a is shown a countercurrent distribution analog to simulate the moving boundary Schlieren sedimentation pattern of a system of four species with formation constants for the monomer-dimer interaction equal to 0.001, 0.154, 10, and 1000 l/g, a total concentration of 16 g/l, and individual concentrations of 6,2,2 and 6 g/l. For this mixture, $\bar{\alpha}_w = 0.5051$, giving $K_{app} = 0.1213$ l/g [3]. The volume of reaction is assumed to be 141.62 ml/mol dimer. Although some resolution is shown in the intermediate region of the pattern, the effect of the raised baseline is apparent.

Figs. 4–6 repeat simulations to illustrate what would happen if it were possible to extract samples from different regions of the sedimentation pattern in fig. 3a. The sample imagined for fig. 4 includes the entire region of fig. 3a containing the slowest peak, the concentration being averaged from direct computer output. The locations of the fractions being considered are illustrated in the concentration diagram shown in fig. 3b. It is seen in fig. 4 that the material from the slowest peak in fig. 3a reproduces itself in position and peak shape: it 'runs true'. It should be noted that in the Gilbert theory [6] for the sedimentation of a self-reacting system, the location or corresponding sedimentation coefficient in a pattern is, for a given formation constant, a single-valued function of concentration: it is a fundamental characteristic that samples must run true when reexamined under identical conditions. Each species in a microheterogeneous system is assumed to be in itself a homogeneous self-reacting system. Then, at any concentration less than that of the plateau region

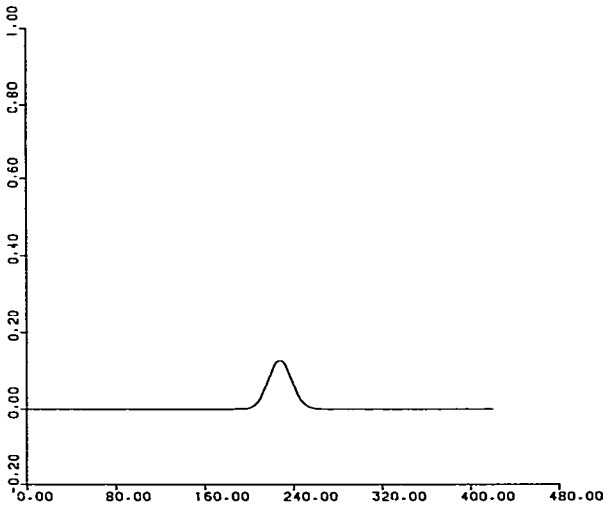

Fig. 4. Countercurrent analog simulation of the resedimentation of the fraction taken from the slow peak of fig. 3a; tube numbers 201–262; concentration, 3.375 g/l.

for that homogeneous system, a given concentration can only be found at one point in the ultracentrifuge cell. As a result, a composite microheterogeneous system of whole and half molecules made up of species which do not interact with each other behaves as follows: at a given time of centrifugation at a given speed, a specified point in the ultracentrifuge cell can contain one and only one distribution of all these species, determined by the original distribution of amounts of materials with specified K values. Hydrodynamic dependence of sedimentation coefficient values on concentration is not included in this argument. The material in fig. 4 is heavily weighted with the species having the smallest assigned formation constant. In fig. 5, it is imagined that a fraction has collected everything between the two principal minima adjoining the slowest and fastest peaks, in fig. 3a. This material must therefore be a mixture which is depleted primarily of the species having the highest assigned formation constant. Again, fig. 5 shows essentially that this is the case. In fig. 6, it is imagined that a fraction has been rerun which was collected from the region in fig. 3a surrounding the fast peak. Since fractions in moving boundary experiments contain all material whose representative boundaries lie above the location of collection, the material in fig. 6 should contain all species in the original sample, with some enrichment of the slower moving species. This is evident in the pattern shown in fig. 6. No matter how many times such a sample is rerun, it will always reproduce the same pattern, since all the species contained are at equilibrium initially, and they each reequilibrate with changing local concentration during the sedimentation experiment in a wholly reproducible way.

In table 2 are shown the composite thermodynamic stopped-flow dilution amplitudes, as calculated for a 10% drop in concentration, from eq. 1, for the three fractions represented in figs. 4–6. These are compared with calculated amplitudes for the original mixture, at the three different concentrations, corresponding to those of the fractions. It is seen that each mixture is predicted to be reactive in stopped-flow dilution experiments, although the amplitude contributions from the species with the lowest and highest formation constants will be relatively small.

To approach the grossly microheterogeneous

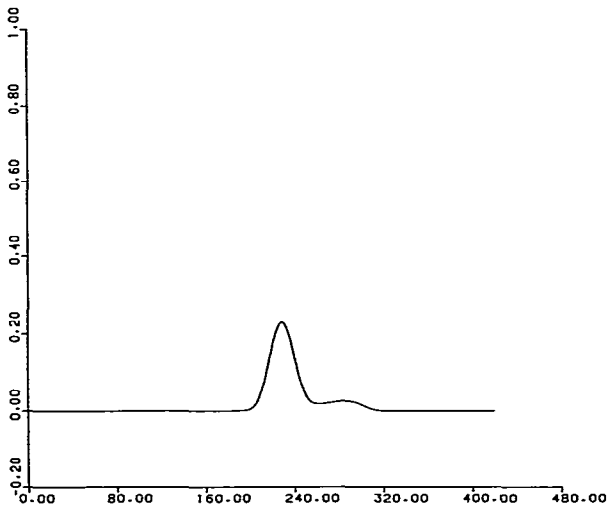

Fig. 5. Countercurrent analog simulation of the resedimentation of the middle fraction of fig. 3a; tube numbers 263–334; concentration, 7.605 g/l.

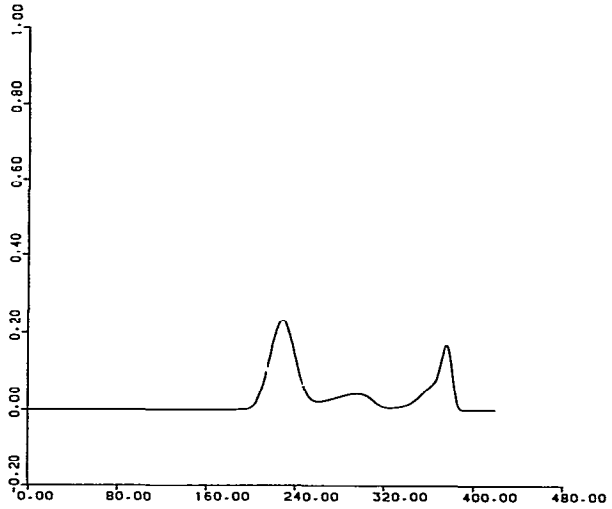

Fig. 6. Countercurrent analog simulation of the resedimentation of the bottom fraction of fig. 3a; tube numbers 335–400; concentration, 11.584 g/l.

Table 2

Thermodynamic dilution reaction amplitudes for four-species mixtures

	Fraction 1 [a]	Control 1	Fraction 2 [b]	Control 2	Fraction 3 [c]	Control 3
Amplitude	7.674×10^{-3}	1.473×10^{-2}	3.532×10^{-2}	1.564×10^{-2}	1.832×10^{-2}	1.639×10^{-2}

[a] Fig. 4.
[b] Fig. 5.
[c] Fig. 6.

Table 3

Fraction assignable to 'half molecules' in five species systems

	Concentration (g/l)				
	3	6	12	24	30
Fraction of 'half molecules'	0.5433	0.5092	0.4713	0.4392	0.4245

behavior discussed by Siezen and Van Driel [2] and Engelborghs and Lontie [8], we have chosen a system with five species, having assigned formation constant values of 0.001, 0.08, 0.3, 2.0 and 1000 l/g, at relative mass concentrations in the ratios 9,2,2,2 and 9, respectively. Moving boundary sedimentation simulations have been developed for total concentrations of 3, 6, 12, 24 and 30 g/l. These have included pressure dependence effects corresponding to 141.62 ml/mol dimer, for each species. For this mixture, $\bar{\alpha}_w = 0.5433$, giving $K_{app} = 0.06448$ l/g [3].

In table 3 are shown values of the fractional concentration assignable to 'half molecules' [2,7], by reading computer output for concentrations to the minimum beyond the slow peak, and taking the ratio to the assigned concentration. The total concentration which would be measured to the plateau region in the presence of a pressure effect favoring dissociation is slightly elevated, as discussed further below, both with time and with ultracentrifuge speed, above that in the original sample, adding some uncertainty to such determinations. Table 3 shows that the experimenter working with such a system should find a smaller drift in the concentration ratio of 'half' to 'whole' molecules with changing concentration than one could explain with reequilibration in a homogeneous reacting system.

Similar computations with identical parameters, except for zero volume of reaction, lead to extremely small differences.

The effect of changing total concentration can be discussed further with the aid of the concentration gradient patterns simulated at 6 and 24 g/l, shown in fig. 7. In both patterns, it is seen that the

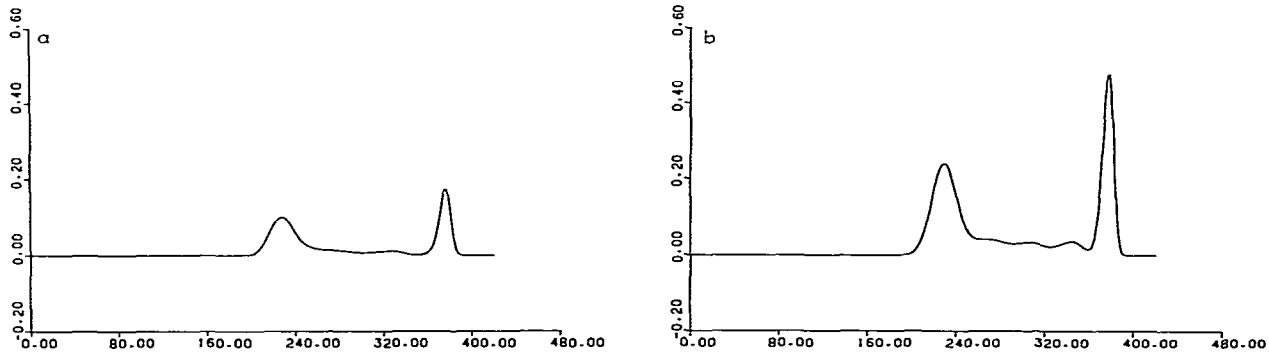

Fig. 7. Countercurrent analog simulations of the sedimentation of a mixture of five species (see text and table 3). (a) Loading concentration 6 g/l. (b) loading concentration 24 g/l.

baseline is elevated between the two major peaks. While some resolution is apparent at the higher concentration, in the intermediate region this effect is appreciably diminished at the lower concentration. In particular, it is seen that there is no large qualitative change in the overall appearance of these patterns over this 4-fold range of concentration. The baseline elevation is retained at either concentration, and there is no very marked shift of the pattern to regions of lower sedimentation rates with decreasing concentration. It is evident by comparing figs. 3 and 7, that as one continues to increase the inherent microheterogeneity of the system (by assigning further species with intermediate formations constants), resolution between the two major peaks continues, as does the elevation of the baseline between them, with a smoothing out of the resolution of intermediate peaks.

The effect of pressure-favored dissociation on raising the concentration in the 'plateau region' is interesting. This effect is still quite small for the volume of reaction selected here, 141.62 ml/mol dimer molecules. However, the concentration level in the plateau region increases with time and speed of centrifugation. This is readily understood by considering the movement into and out of a thin lamina in the plateau region, for a single homogeneous reacting species. At the upper edge of the lamina, where the pressure is lower, the ratio of dimer to monomer is higher, for a given concentration, than that at the lower edge of the lamina, were higher pressure has caused dissociation. Consequently, there is an excess influx of material, which shows up as an increase of concentration with time in the plateau region. This argument says nothing about possible total concentration gradients in this region, except that there must be a positive gradient of monomer and a negative gradient of dimer with increasing radius of rotation. In the examples studied, even at much higher positive volumes of association, no cases have been seen in which there is a large positive gradient of total concentration with radius of rotation in the plateau region.

Finally, fig. 8 illustrates a further problem in understanding the nature of heterogeneous mixtures such as those which have been considered.

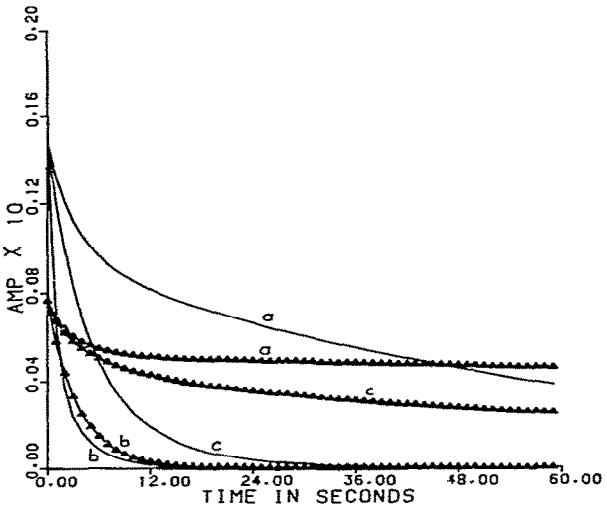

Fig. 8. Predicted composite relaxation curves from stopped-flow 10% dilution of a system of four species. Formation constants as in fig. 3, and predicted thermodynamic amplitudes in table 2. (a) Association rate constants identical at 0.0409 l/g per s. (b) dissociation rate constants identical at 0.26558 s^{-1}. (c) association and dissociation rate constants all differ, according to table 4. (———) Original unfractionated material, diluted from 3.375 g/l. (▲———▲) Fraction (fig. 4) recovered from the slow peak in fig. 3a, diluted from 3.375 g/l.

Even when equilibrium constants and relative concentrations have been postulated for individual monomer-dimer reacting species composing a microheterogeneous system, and both the thermodynamic stopped-flow dilution amplitudes and the predicted sedimentation patterns can be established, based on the assumption of rapid equilibration of all species, one must guess at various combinations of association and dissociation rate constants to complete the picture. For the four-species mixture examined in fig. 3, one could make two extreme assumptions: (1) all of the association rate constants for the four species are identical, and the dissociation rate constants contain all of the differences which are associated with the four different equilibrium constants; or (2) all of the dissociation rate constants are identical and the differences in equilibrium constants are caused only by corresponding differences in the association rate constants. Additionally, one could make

any number of assumptions in which both association and dissociation rate constants are different for all four species, consistent with their differing equilibrium constants. Predicted stopped-flow dilution relaxation patterns for these two extreme assumptions and one intermediate assumption are shown in fig. 8. The prediction of the single relaxation for each homogeneous species is based [14] on the equation

$$1/\tau^2 = 4k_f k_r c + k_r^2 \quad (3)$$

where τ is the relaxation time, k_f and k_r the association and dissociation rate constants, respectively, and c the weight concentration. In each simulated mixture, at least one species is chosen to have the association rate constant of 0.0409 l/g per s, consistent with the equilibrium [3,8] and kinetics [9] observations at pH 5.7 in the presence of 0.4 M NaCl, where the fastest kinetics have been observed [1]. It is seen that for the constant association rate constant assumption, composite slow relaxation processes are predicted for the original mixture of four species (curve a). This prediction is inconsistent with experiments at pH 5.7. On the other hand, for the constant dissociation rate constant assumption, the predicted relaxation curves agree more closely with the results of fractionation experiments and stopped-flow experiments [1]. The experimental results indicated that supernatant fractions exhibited stopped-flow dilution amplitudes less than those of original material. Much the same discussion applies to the one case shown, in which both the association and dissociation rate constants vary from species to species, in accordance with their equilibrium constants (table 4).

These two possible kinetic rate constant assumptions illustrated in fig. 8 are each consistent with recorded experiences for *H. pomatia* α-hemocyanin under various conditions [1,2,7,8], and the results of this study. Thus, it is possible to say with some degree of confidence that if microheterogeneity in formation constants accounts for the nature of the whole-half molecule resolution in moving boundary sedimentation, as described above, then the individual monomer-dimer reactions are reasonably fast, and the differences in formation constants cannot be ascribed solely to differences in dissociation rate constants.

Table 4

Rate constants used in fig. 8 (curves c)

k_f (l/g per s)	k_r (s^{-1})	K (l/g)
3.2958×10^{-3}	3.2958	10^{-3}
4.09×10^{-2}	2.6558×10^{-1}	0.154
3.2958×10^{-1}	3.2958×10^{-2}	10
3.2958	3.2958×10^{-3}	10^{+3}

3. Summary

The model employed for the present simulations assumes the presence of extensive microheterogeneity, in agreement with previous studies [2,7,8]. However, it is further assumed in this extended model that all component species are fairly rapidly reequilibrating, with reaction amplitudes and sedimentation behavior explainable by variations in individual whole molecule formation constants. It is emphasized that whole molecules are capable of exhibiting reaction amplitudes on dilution over an extremely wide range of formation constants, so that incompetent whole molecules [3] might be more exactly defined as those with a formation constant-concentration product larger than 10^4.

References

1 R.J. Siezen, E.F.J. van Bruggen, M.-S. Tai, M.C. Crossin and G. Kegeles, Biophys. Chem. 19 (1984) 99.
2 R.J. Siezen and R. van Driel, Biochim. Biophys. Acta 295 (1973) 131.
3 G. Kegeles, Arch. Biochem. Biophys. 180 (1977) 530.
4 J.R. Cann and G. Kegeles, Biochemistry 13 (1974) 1868.
5 J.R. Cann, Interacting macromolecules (Academic Press, New York, 1970).
6 G.A. Gilbert, Disc. Faraday Soc. 20 (1955) 68.
7 W.N. Konings, R.J. Siezen and M. Gruber, Biochim. Biophys. Acta 194 (1969) 376.
8 Y. Engelborghs and R. Lontie, J. Mol. Biol. 77 (1973) 577.
9 M.S. Tai, G. Kegeles and C.H. Huang, Arch. Biochem. Biophys. 180 (1977) 537.
10 J.L. Bethune and G. Kegeles, J. Phys. Chem. 65 (1961) 1761.
11 G. Kegeles, L.M. Rhodes and J.L. Bethune, Proc. Natl. Acad. Sci. U.S.A. 58 (1967) 45.
12 M.-S. Tai and G. Kegeles, Arch. Biochem. Biophys. 142 (1971) 258.
13 K.E. Van Holde, D. Blair, N. Eldred and F. Arisaka, in: Structure and function of hemocyanin, ed. J.V. Bannister (Springer-Verlag, Berlin, 1977) p. 22.
14 M.-S. Tai and G. Kegeles, Biophys. Chem. 3 (1975) 307.